A Batteryless Vibration-based Energy Harvesting System for Ultra Low Power Ubiquitous Applications

Lu Chao, Chi-Ying Tsui and Wing-Hung Ki
Department of Electronic and Computer Engineering
The Hong Kong University of Science and Technology
Hong Kong SAR., P. R. China
{eeluchao, eetsui and eeki}@ee.ust.hk

***Abstract*—In this paper, we propose a vibration driven energy harvesting platform based on piezoelectric material. A new maximum power point tracking (MPPT) method for this platform is also presented. This platform harvests ambient vibration energy as its power source, and is capable of self-starting, and self-powered operation without the need of a battery. The proposed MPPT methodology consumes very little power, and is especially suitable for the environments, where ambient harvested power is very low. System modeling, analysis, and implementation are developed. Simulation results show that the power harvesting efficiency with the proposed MPPT scheme is higher than 90% and the power utilization efficiency of the overall platform is higher than 50%.**

I. INTRODUCTION

Recently, the concept of ubiquitous computing, sensing, and perception has drawn a lot of attention in the research community. Computation is embedded into environments to facilitate the interaction among devices and human naturally and causally. One example is wireless sensor network, which has potential to be used in many areas. The conventional solution for providing the required power to each sensor node is to use electrochemical batteries. However, battery is bulky, costly and difficult to replace regularly in many applications. This poses a big limitation on the deployment of such systems. In some ultra low power applications (e.g. picoradio [1], smart dust [2]), which demand low cost, long lifetime, small volume and light weight, eliminating the battery is desirable.

For some ubiquitous applications, the average power consumption can be down to the level of tens to hundreds of micro watts. In this case, energy harvested from environments can be used as an alternative power source to provide a virtually infinite lifetime[3][4]. Mechanical energy conversion is one of the common sources for these energy harvesting applications. Low level vibrations commonly occur in household or industrial environments. It is estimated that mechanical vibrations inherent in the environment can provide a power density of tens to hundreds of micro watt per cm^3, which is sufficient to sustain operations of a sensor node [5]. In this work, we focus on the energy harvesting systems using piezoelectric conversion. Previous studies have found that for piezoelectric material, under a given vibration status (magnitude and frequency), there is an optimal output voltage point where maximum harvested power can be achieved [7]. Vibration status is heavily dependent on the environment where the applications are located. In reality, because of the time-varying nature of the environments, vibration status is often unstable and varying. Consequently, the optimal voltage point is also changing. In order to harvest as much energy as possible, a run-time adaptive mechanism is required to track the optimal output voltage with the environmental changes. At the same time, this tracking mechanism should have as low power overhead as possible since the energy harvested is already very small.

A vibration based self-powered wireless sensor using a fixed voltage band-band control was proposed [6]. A vibration energy harvesting system was presented in [7], where MPPT was controlled by a DSP through comparing the harvested power before and after a change in the duty cycle of a buck converter. The power overhead of the MPPT mechanism was not presented. A simpler control method and controller was developed in [8]. The reported power overhead of the MPPT controller is 5.74mW and it may not be suitable for low power ubiquitous applications such as wireless sensor networks, which are deployed in environments with only low level vibrations. In these cases, the harvested power is very low and is in the range of tens to hundreds of micro watts. Thus, to cater for low level vibration environments, it is necessary to develop a new MPPT method, which has very little power loss and the corresponding circuit implementation is simple.

In this paper, we tackle the above two design challenges. We propose a novel MPPT scheme that has a very low power overhead, which is in the order of microwatts. This is about three orders of lower than the existing MPPT approaches. Based on this MPPT scheme, a battery-less vibration based energy harvesting system is presented. It was implemented using 0.35μm CMOS process. Overall system simulations were carried out to verify the functionality and behavior of the system. Simulation results show that the power harvesting efficiency with the proposed MPPT scheme is higher than 90% and the power utilization efficiency of the overall system is higher than 50%.

II. THE PROPOSED MPPT SCHEME

A. Electrical Model of the Piezoelectric Film

We use a commercial piezoelectric thin film [9] and its equivalent electrical model is shown in Fig. 1a. It consists of a

This work was supported in part by the Hong Kong Research Grants Council under Grant CERG 620305

sinusoidal current source i(t)=$I_p$sin(2πft) where I_p depends on the vibration magnitude, f is the vibration frequency, C_p and R_p are the internal capacitance and resistance, respectively. Measurement results show that C_p is almost constant under a wide range of vibration frequencies. R_p is usually very large and can be ignored. The output voltage of a piezoelectric film depends on the material's geometry, piezoelectric properties, the mechanical vibration strength, and the output impedance.

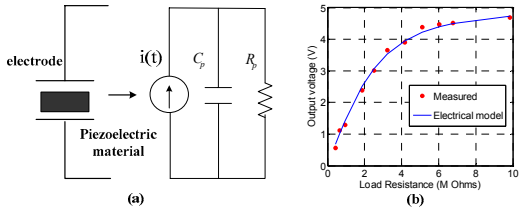

Figure 1. (a) Piezoelectric film model (b) experimental validation

Experiments were conducted to validate the electrical model. A piece of 1.3cm×2.5cm×0.2mm piezoelectric film with C_p=0.5nF was amounted on a variable vibration platform. Various resistive loads were connected to the film and the peak-to-peak output voltages were recorded. Fig. 1b shows the measured output voltages and the simulated output voltages using the equivalent electrical model for different output loading. It can be seen that the electrical model matches well with the measurement data. In the following analysis, we will use this current source model.

B. Maximum Harvested Power

The output of the piezoelectric film is an AC voltage signal. For energy harvesting, we need an AC-DC rectifier to convert it to DC voltage. Fig. 2 shows the equivalent electrical model of the piezoelectric film with the rectifier. The instantaneously harvested power is small and may not be able to sustain continuous operations of the application. The capacitor C_s is inserted to accumulate the harvested power. The time-averaged harvested current $<i_o(t)>$at the output of the rectifier and the time-averaged harvested power <p(t)> are given by

$$< i_o(t) >= \frac{2I_p}{\pi} - \frac{4(Vs + 2\Delta V)\pi f C_p}{\pi} \quad (1)$$

$$< P(t) >= \frac{2I_p Vs}{\pi} - \frac{4Vs^2 \pi f C_p}{\pi} - \frac{8Vs\Delta V \pi f C_p}{\pi} \quad (2)$$

where ΔV is the forward voltage drop of the diode. Maximum power can be obtained at the output if

$$Vs = \frac{I_p}{4\pi f C_p} - \Delta V \quad (3)$$

and we denote the value of V_s as the optimal output voltage value. From (3) we can see that the optimal voltage for maximum power harvesting depends on the vibration magnitude I_p and frequency f, which are not constant and are varied with the practical environment and time. Thus the maximum power point is also changing with the vibration status. We simulated the harvested power with different vibration status and plotted the results in Fig. 3. It can be seen that the optimal V_s point varies significantly. To achieve a maximum harvested power, we need to track this optimal voltage point with very little power overhead.

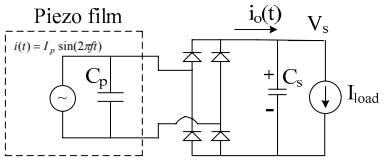

Figure 2. Energy harvester

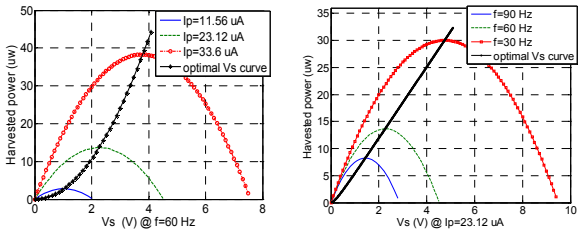

Figure 3. Harvested power versus output voltage points

C. Vibration Tracking

We propose a time-multiplexing mechanism for MPPT. The output of the piezoelectric film is periodically disconnected from the application and connected to a vibration tracking unit to track the optimal V_s. The operation of the vibration tracking unit is described in the following. If a resistive load R is connected to the output of a piezoelectric film, as shown in Fig. 4a, its instantaneous and peak output voltage are given by

$$V_o = I_p \frac{R}{\sqrt{1 + (2\pi f R C_p)^2}} \sin(2\pi f t + \theta) \quad (4)$$

$$V_{o,peak} = \frac{I_p}{2\pi f C_p} \qquad \text{if } (2\pi f R C_p >> 1) \quad (5)$$

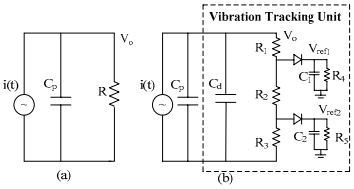

Figure 4. Vibration tracking unit

Comparing (3) and (5), we can see that V_s=$V_{o,peak}$/2-ΔV, so we can obtain the value of V_s from $V_{o,peak}$. Based on this, we propose an architecture for tracking V_s and hence the vibration, as shown in Fig. 4b. It is only composed of simple passive elements and its operation does not require a battery. Since the peak voltage of the AC signal generated from the piezoelectric film can be very large, it is not suitable to directly use this voltage value for the control circuit. As shown in Fig. 6a, the control unit uses V_s as the supply voltage and V_{ref1}, V_{ref2} are the input signals, so V_{ref1} and V_{ref2} have to be reduced to less than V_s for correct operation. Here, we reduce the values of V_{ref1} and V_{ref2} by adding an extra capacitor C_d (C_d=C_p) and a resistor string (R_1,R_2, R_3) across the output of the piezoelectric film. The equivalent R value (R_1+R_2+R_3) is large enough to satisfy the condition of $2\pi fR(C_p+C_d)>>1$. Consequently, $V_{o,peak}$ = I_p/[2πf(C_p+C_d)] = I_p/4πfC_p is obtained. Through the voltage divider and low pass filters, the voltages across the capacitor C_1, and C_2 are

$$V_{ref1} = \frac{I_p}{8\pi f C_p} - \Delta V + \sigma \quad V_{ref2} = \frac{I_p}{8\pi f C_p} - \Delta V - \sigma \quad (6)$$

where ΔV is the forward voltage drop of the diode and σ is a very small voltage roughly given by $R_2/(R_1+R_2+R_3)$. V_{ref1} and

V_{ref2} are then sent to the control circuit to maintain the output voltage to be the optimal voltage point.

III. VIRBRATION-BASED ENERGY HARVESTING SYSTEM

Fig. 5 shows the block diagram of the proposed vibration based energy harvesting system. MOS switches N_1 and P_1 are used to implement the time-multiplexing MPP Tracking. Since the vibration variation will not be very fast, we do not need to continuously track the vibration status. So periodically the vibration tracking unit is connected to the piezoelectric film. The duty cycle directly affects the time that the piezoelectric film can be used for energy harvesting. Therefore, the duty cycle has to be very small to reduce the power overhead. Here we use a duty cycle of 1%. The output of the vibration tracking unit are sent to the control unit to turn on/off the switch S_1 to supply the current to the load and to keep the V_s at the optimal voltage value. The design of the control unit will be discussed in the following sub-section. A buck converter is used to convert the unregulated input voltage V_s into a regulated output voltage V_{out}, which is the required operation voltage of the application. V_s is the supply voltage for the control unit, the pulse generator and buck converter. If the harvested power is larger than the power loss of these three blocks, the system can be self-powered without the need of a battery.

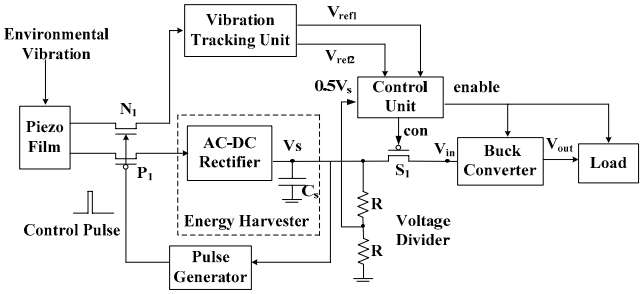

Figure 5. Block diagram of the proposed batteryless vibration-driven energy harvesting system

A. Control Unit

The control unit implements a band-band control strategy to maintain the output voltage of the energy harvester at the optimal voltage value. It mainly consists of a Schmitt trigger and a voltage comparator, as shown in Fig. 6a. Two control signals "con" and "enable" are generated to turn on/off the switch S_1 to keep the output voltage and to enable the application, respectively. When C_s is charged up to a value higher than $2V_{ref1}$, "con" becomes low and turns on S_1. Then the application wakes up from sleep mode and starts an atomic operation. Power is transferred to the application through the buck converter. When V_s is decreased to $2V_{ref2}(1+R_1/R_2)$, "enable" becomes low to disable the application, which should store the operation state for next operation before going to sleep mode again. When V_s is lower than $2V_{ref2}$, "con" becomes high and turns off S_1, and one operation round is finished. Once the harvested power charges up C_s and V_s reaches $2V_{ref1}$, the operation cycle repeats again.

The speed of the control unit does not need to be very high and power loss is the most significant parameter to achieve a low power overhead. The comparators are designed to be operated in subthreshold region [10], as shown in Fig. 6b. It contains a two-stage operational amplifier and a current source, where the bias current remains constant with the power supply changes. Thus, it is guaranteed that the bias current of the amplifier is small enough for normal subthreshold operation.

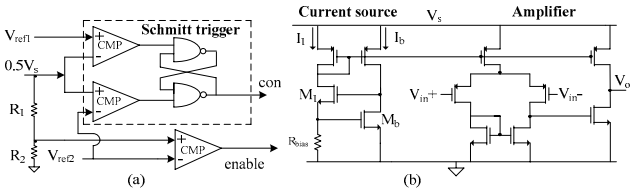

Figure 6. (a) Control unit diagram (b) Comparator architecuture

B. System Start-Up

During starting, there are low level vibrations occurring at the piezoelectric film. Initially, V_s is zero and can not drive the operation of the pulse generator. The output of the pulse generator remains at zero. Thus, the switch N_1 is off and P_1 is on, and the harvested current from the piezoelectric film only flows into the storage capacitor C_s. The harvested power charges up C_s, and V_s is increasing. When V_s is high enough to drive the pulse generator to generate the periodic control pulse, the corresponding V_{ref1} and V_{ref2} are generated from the tracking unit. This time instance is marked as t in Fig. 7. From then on, the system begins the regular operations.

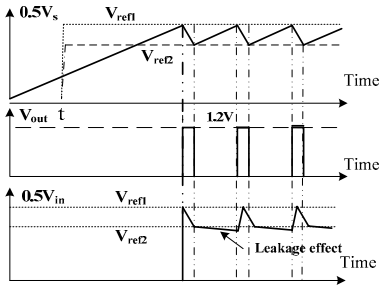

Figure 7. Illustrative graphs for overal system operation

C. Regular Operations

The operation mechanism of the proposed system is illustrated in Fig. 7. In each operation cycle, the energy transferred to the buck converter and the load can be estimated as $E=2C_s(V^2_{ref1}-V^2_{ref2})$. C_s should be sized such that it is large enough for the execution of an atomic operation of the application even under the worst case (i.e. the lowest allowable output voltage from the rectifier).

IV. SIMULATED RESULTS

The proposed energy harvesting system was implemented in AMS 0.35μm CMOS technology. We used a piezoelectric film with the dimension 1.6cm*6.15cm*1mm. C_p is 11.12nF and C_s is 60μF. A 47μH inductor was used for the buck converter. The output voltage of the buck converter is set to 1.2Vwith the ripple voltage less than 25mV. The power consumption of the load is assumed to be 72μW.

Various simulations were conducted to verify the tracking performance of the MPPT mechanism and the power harvesting performance of the system. The first set of experiment was carried out to demonstrate the tracking performance. Different sets of vibration status (I_p=15μA~55μA, f=25Hz~90Hz) were used. For each set of vibration status, theoretical maximum power point was

achieved by using the corresponding optimal resistive load as the load. For the proposed MPPT scheme, we carried out HSPICE simulations on the circuit to find the optimal voltage. Power overhead was included in the simulations. The system using a fixed voltage band-band control scheme was also simulated and plotted for comparison. Here, V_{ref1} and V_{ref2} are fixed at 2.51Vand 2.49V, respectively.

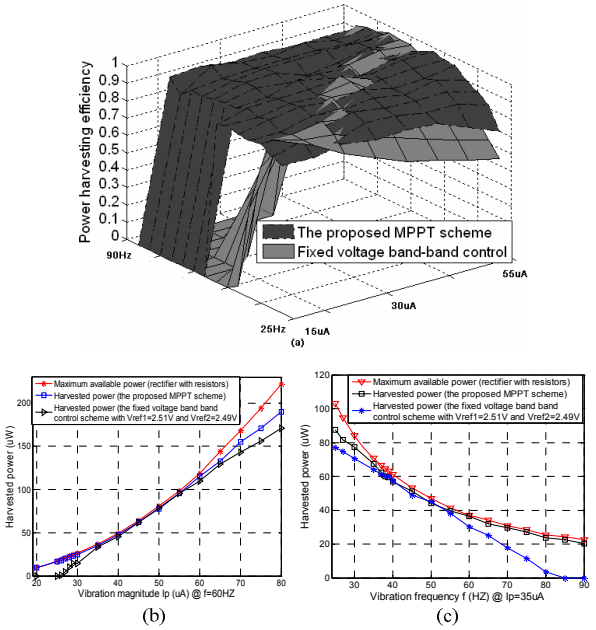

Figure 8. (a) Power harvesting efficiency (I_p=15μA~55μA, f=25Hz~90Hz) (b) Harvested Power @ f=60 Hz (c) Harvested Power @ I_p=35μA

The power harvesting efficiency is defined as the ratio of the actually harvested power divided by the theoretical maximum harvested power from the energy harvester. Fig. 8a plots a 3D graph showing the relationship between the power harvesting efficiency and the vibration status. When f is high and I_p is low (e.g. f=90Hz, I_p=15μA), the maximum available voltage on the energy harvester is less than the system minimum allowable voltage. The system can not operate and the power harvesting efficiency is zero. As f decreases or I_p increases, the system can operate well and we can find that in most of vibration status configurations, the proposed MPPT scheme, whose power harvesting efficiency is around 90%, outperforms the fixed voltage control scheme. Fig. 8b and 8c show the tracking performance when one of the vibration parameters is fixed. We can see that most of time, the proposed MPPT scheme tracks well with the theoretical optimal point. If the optimal voltage value is large, the proposed scheme has a lower power harvesting efficiency due to the increasing power overhead of the MPPT implementation which increases with the output voltage.

Fig. 9 shows the simulation waveforms of V_s and V_{out} of the buck converter for a given vibration status (f=60Hz, I_p= 35.6μA). Under this vibration scenario, the maximum power harvested by the energy harvester is 38.35μw, with the optimal voltage V_s=3.84V. The cycle time of each regular operation is 1.162s and the operation time of the load per cycle is 0.319s. The power harvested with the proposed MPPT scheme is 36.79μW, which means the power harvesting efficiency is 95.93%. The power utilization efficiency is defined as the ratio of the average power delivered to the load divided by the theoretical harvested power from the energy harvester. In this scenario, the average power delivered to the load is 19.938μW, and the power utilization efficiency is 51.99%. Note that the power utilization efficiency includes the conversion efficiency of the buck converter which has a relatively large loss.

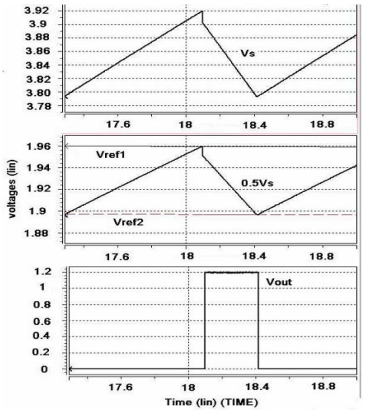

Figure 9. Simulated overall system waveforms

V. CONCLUSION

To dynamically track the maximum input power point from the time-location-varying environmental vibrations, we propose a new MPPT scheme which has extremely low power overhead. We also propose a batteryless vibration driven platform for low power ubiquitous applications. This platform is capable of completely self-powered by the harvested energy and starting up automatically. Circuit implementation and simulations were carried out to verify the power tracking performance and the feasibility of the proposed platform.

References

[1] J. Rabaey, J. Ammer, T. Karalar, S. Li, B. Otis, M. Sheets, T. Tuan, , "PicoRadios for Wireless Sensor Networks: The Next Challenge in Ultra-Low-Power Design", Proceedings of the International Solid-State Circuits Conference, San Francisco, CA, February 3-7, 2002.

[2] "Smart dust": Brett Warneke, Bekeley user archive, April 30, 2004 www.bsac.eecs.berkeley.edu/archive/users/warneke-brett/SmartDust

[3] L. Mateu, F. Moll, "Review of energy harvesting techniques and applications for microelectronics", the Proceedings of the SPIE Microtechnologies for the New Millenium, pp.359-373, 2005

[4] S. Roundy, P. K. Wright, J. Rabaey, "A study of low level vibrations as a power source for wireless sensor nodes", computer communications, vol.26, no.11, pp. 1131-1144, 2003

[5] S. W. Arms, C. P. Townsend, D. L. Churchill, J. H. Galbreath, and S. W. Mundell, "Power management for energy harvesting wireless sensors", SPIE Int'l Symposium on Smart Structures and Smart Materials, San Diego, CA, March 9, 2005

[6] Eli S. Leland, Elaine M. Lai, Paul K. Wright, "A self-powered wireless sensor for indoor environmental monitoring", 2004 Wireless Networking Symposium, 2004

[7] G. K.Ottman, A. C. Bhatt, H. Hofmann, and G.A. Lesieutre, "Adaptive piezoelectric energy harvesting circuit for wireless remote power supply", IEEE Transaction on power electronics, vol.17, 2002

[8] G.K.Ottman, A. C. Bhatt, H. Hofmann, and G.A. Lesieutre, "Optimized piezoelectric energy harvesting circuit using step-down converter in discontinuous conduction mode", IEEE Transaction on Power electronics, pp.696-703, 2003

[9] Measurement Specialties, technical manual for piezoelectric film, http://www.meas-spec.com/.

[10] Triet T. Le, Jifeng Han, Annette von Jouanne, Kartikeya Mayaram, and Terri S. fiez, "Piezoelectric micro-power generation interface circuits", IEEE Journal of Solid-State Circuits, Vol.41, No.6, June 2006